Mar Biol (2016) 163:208
DOI 10.1007/s00227-016-2983-y

ORIGINAL PAPER

Oxygen transport in periodically ventilated polychaete burrows

Elizabeth A. K. Murphy[1] · **Matthew A. Reidenbach**[1]

Received: 15 April 2016 / Accepted: 6 September 2016 / Published online: 17 September 2016

Abstract Burrowing organisms play a critical role for the functioning of coastal marine sediments, in part due to their pumping of oxygenated water through the burrow. In cohesive sediments, oxygenated burrow water allows for the diffusive flux of oxygen across the burrow wall and into the sediment, where it is consumed. In this study, we quantified the burrow excurrent velocities, volume of water ventilated and oxygenation patterns within the burrow of the polychaete *Alitta succinea.* We determined that periodic ventilation of the burrow results in oscillations of the flux of oxygen across the burrow wall and oxygen concentration within the sediment near the burrow wall. Additionally, we investigated the effects of temperature changes on oxygen dynamics in the burrow. The volumetric flow rate and frequency of burrow ventilation increased with temperature. Correspondingly, the frequency of the oscillations in oxygen flux across the burrow walls also increased with temperature. However, the time-averaged flux of oxygen across the burrow wall did not change with temperature (1.5 ± 0.3ol m^{-2} d^{-1}), and the distance of oxygen penetration into the burrow wall decreased with temperature (from 3.4 ± 0.5 at 6 °C to 1.6 ± 0.1 at 33 °C). Thus, seasonal changes in the volume of oxygenated sediment, as well as the pattern of oxygenation that sediment experiences, are expected to be significant while the total oxygen flux is expected to remain relatively uniform. We show that burrower ventilation behavior mediates the effects of temperature on sediment oxygen uptake.

Responsible Editor: M. Huettel.

Reviewed by undisclosed expert.

Electronic supplementary material The online version of this article (doi:10.1007/s00227-016-2983-y) contains supplementary material, which is available to authorized users.

✉ Elizabeth A. K. Murphy
eam6vf@virginia.edu

[1] Department of Environmental Sciences, University of Virginia, Charlottesville, VA 22904, USA

Introduction

Sediments play a critical role in the cycling of nutrients and carbon in marine systems (Boudreau and Jørgensen 2001). Within coastal sediments, a rich array of burrowing organisms, such as ghost shrimp, razor clams, polychaete worms and nemerteans, burrow to seek refuge from predation and in search of food (Wilson 1990). Marine sediments, ranging from muds to sands, possess specific mechanical properties. Muds are characterized as cohesive sediments due to the organic mucopolymer matrix that binds sediment grains (Dorgan et al. 2006), preventing advective transport of solutes in low-permeability muddy sediments (Glud 2008). Sandy sediments are typically permeable, allowing advective pore water transport (Janssen et al. 2005).

Many types of burrowing animals build permanent or semipermanent burrows flushed with overlying water. Stagnant burrow water is quickly depleted of oxygen, due to the respiration of the burrower and microbes that live within the burrow walls (Kristensen 1985). In order to maintain a favorable chemical environment, many burrowers flush their burrows with overlying, oxygenated water, a process referred to as burrow ventilation. Some animals also ventilate their burrows for other reasons, including feeding, removal of toxic metabolites or irritants, release of gametes, and environmental sensing (Wells and Dales 1951; Riisgård 1989; Kristensen and Kostka 2005; Smee and Weissburg 2006). In cohesive, low-permeability sediments,

burrow ventilation results in enhanced diffusive transport of solutes between sediments and the water column by increasing the surface area available for diffusion, in some cases by as much as 400 % (Ziebis et al. 1996). Solute transport between the water column and sediments due to burrow ventilation is known as bioirrigation (Kristensen et al. 2012), and this process has important biogeochemical consequences. Enhanced microbial breakdown of organic matter in bioirrigated sediments is a result of increased numbers of microbes and meiofauna, with higher numbers of microbes often found in oxic burrow walls than at either the sediment surface or anoxic subsurface sediments [e.g., nereidid burrow walls have an increase in bacterial abundance of 2.7–4.5 times the surrounding ambient sediment, depending on the species (Papaspyrou et al. 2006)]. This also results in enhanced nutrient cycling and regeneration (Kristensen 2000; Karlson et al. 2005), such as an increase in nitrate fluxes from the sediment in the presence of burrowers, dependent on ventilation behavior (Henriksen et al. 1983), and three–fivefold increases in ammonium fluxes out of the sediment, dependent on burrow density (D'Andrea and DeWitt 2009).

Oxygen is typically diffusion limited in cohesive marine sediments, and therefore, these sediments are anoxic below a thin layer (on the order of a few millimeters) at the sediment surface that is supplied with oxygen by diffusion (Gundersen and Jørgensen 1990). Oxygen is depleted within the sediment due to the consumption of oxygen during microbial respiration or the oxidation of reduced compounds (Jørgensen and Revsbech 1985; Glud 2008). Burrow ventilation is therefore important for organic matter processing not only because it effectively increases the sediment–water interface, but because the activity also introduces oxygen deep into otherwise anoxic sediments in a spatially and temporally heterogeneous manner. In many coastal sediments, the total oxygen uptake is higher than the diffusive flux of oxygen across the sediment–water interface (Glud et al. 1994, 2003). This discrepancy is typically due to enhanced oxygen uptake mediated by burrowing macrofauna (Meile and Van Cappellen 2003). Organic matter remineralization in marine sediments is primarily due to microbial degradation of organic matter, the rate of which is controlled in large part by the availability of electron acceptors (especially oxygen) and the accumulation of toxic metabolites such as sulfide (Aller and Aller 1998). Burrowing organisms stimulate microbial respiration and therefore rates of organic carbon remineralization, by introducing oxygen into anoxic sediments and flushing out toxic metabolites (Kristensen 2000).

Burrow ventilation is accomplished through different mechanisms by different types of organisms. Many polychaetes use peristaltic or undulating movements to pump water through their burrow, or use cilia to drive water movement (Wells and Dales 1951; Riisgård and Larsen 2005). Many animals that ventilate their burrows do so periodically, alternating between periods of active pumping and periods of rest, with the frequency and duration highly species dependent (Kristensen and Kostka 2005). This intermittent ventilation results in periodic oxygenation of the burrow (Boudreau and Marinelli 1994), and oscillating redox conditions within the burrow wall (Volkenborn et al. 2012a, b). Organic matter is remineralized faster under these intermittently oxic conditions than under constantly oxic or anoxic conditions (Aller 1994).

In this study, we address how burrower pumping behavior influences the pattern of oxygenation in the burrow, and the flux of oxygen across the burrow walls. We hypothesize that increases in the rate of pumping will enhance oxygen transport into the sediments and that the rate of pumping and oxygen transport will vary seasonally due to temperature changes. We chose a common coastal polychaete, *Alitta succinea* (Leuckart 1847; formerly *Nereis succinea*), as our study organism. This species is found in intertidal and subtidal coastal sediments worldwide and has been recorded occurring in densities up to 1600 m^{-2} (Bartoli et al. 2000). It is thought to be introduced in some locations (Carlton 1979), and its presence has been shown to impact sediment biogeochemistry, including oxygen uptake by sediments and denitrification rates (Bartoli et al. 2000). Like many nereidid polychaetes, *A. succinea* builds burrows with at least two openings and periodically ventilates the burrow by undulating its body, with waves passing from the head towards the tail (Kristensen 1981).

Relatively few studies have measured oxygen levels in burrows, and fewer still have measured oxygen fluxes across the burrow wall (Vopel et al. 2003; Polerecky et al. 2006; Pischedda et al. 2012); most studies measure the temporally and spatially averaged oxygen uptake of bioirrigated sediment. This approach neglects to address the underlying oxygen dynamics over small scales in time and space that drive oxygen fluxes into the sediment. Planar optodes are a relatively new instrument that allow for detailed study of oxygen dynamics in marine sediments, highlighting the spatial heterogeneity of oxygen levels in the burrow (Glud et al. 1996), and have been used to measure oxygen fluxes across burrow walls (Pischedda et al. 2008, 2012).

In addition, shallow coastal waters in many regions exhibit high seasonal temperature variability, with temperature affecting the ventilation patterns of many burrowing marine invertebrates (Kristensen 1983; Stanzel and Finelli 2004). Here, we measure pumping behavior and oxygen flux across burrow walls over a range of temperatures, providing insight into how the link between environmental variables, in this case temperature, and sediment–water fluxes are mediated by burrower behavior.

Table 1 Temperature dynamics within the sediment of intertidal mudflats

	3 cm depth ($N = 3$)	10 cm depth ($N = 3$)	20 cm depth
Temperature (°C)			
Mean temp.	16.0 ± 0.1	16.0 ± 0.1	16.0 ± 0.2 ($N = 2$)
Max temp.	33.9 ± 0.9	30.1 ± 0.4	27.4 ± 0.6 ($N = 2$)
Min temp.	−2.1 ± 0.6	−0.7 ± 0.3	1.2 ± 0.9 ($N = 2$)
Variance			
Daily timescale	3.1 ± 0.9	0.9 ± 0.2	0.2 ± 0.1 ($N = 3$)
Weekly timescale	5.2 ± 1.4	2.4 ± 0.4	1.0 ± 0.2 ($N = 3$)
Monthly timescale	9.3 ± 1.5	5.9 ± 0.5	4.2 ± 1.1 ($N = 3$)

Values are mean ± S.E. *N* number of sites measurements were taken at

Within this study, we address four questions: (1) How does the oxygen level vary in the burrow water of intermittently pumping *A. succinea*? (2) How does the magnitude of the flux of oxygen across the burrow walls fluctuate over time? (3) Does the volume and velocity of water pumped through the burrow change with temperature variations typically seen across seasons? (4) Do changes in temperature alter these patterns of oxygenation and oxygen flux? This study aims to link the effects of polychaete pumping behavior with sediment oxygen uptake, and the influence of temperature on both.

Materials and methods

Animal and sediment collection

Specimens of *A. succinea* were collected from intertidal mudflats on the southern Atlantic side of the Delmarva Peninsula, VA, USA. Moderately sized (wet weight between 0.05 and 0.2 g) specimens were chosen for experiments. Animals were kept at room temperature in glass aquaria consisting of mudflat sediments overlain with aerated seawater until use. Sediment for use in experiments was collected from Chimney Pole Marsh (37°27′45.5″N, 75°42′58″W), an intertidal mudflat in the same region where animals were collected. Sediments were collected using a corer, from which a subsample was extracted into the experimental aquaria. The natural structure of the sediment was preserved, and sediment was not used if macrofauna were present. The porosity of the sediment at Chimney Pole was previously measured as 0.70 ± 0.02 vol/vol (McLoughlin 2011).

Field conditions

Submersible temperature loggers (HOBO Pendant Temperature/Light Logger UA-002; Onset Computer Corporation, Bourne, MA, USA) were deployed in three intertidal mudflats similar to that where animals were collected. Three HOBOs were buried at each location, at 3, 10 and 20 cm depth. The temperature within the sediment was measured every 10 min for a year, from September 2013 to September 2014. The 20-cm-depth HOBO at site 2 stopped recording after December 17, 2013 due to a sensor malfunction. The variance in temperature over different timescales (day, week, and month; Table 1) was calculated by dividing the temperature time series from each location at each depth into day-long, week-long and month-long series, then computing the variance for each of these time periods.

Alitta succinea abundance

We determined *A. succinea* population density on two intertidal mudflats on the Delmarva Peninsula similar to those from which animals were collected for the experiment and temperatures were measured. On each mudflat, one sediment core, 25 cm in diameter and 10 cm deep, was taken approximately every 15 m for 75 m along a transect perpendicular to the water line, providing 5 cores per site. Sediment from the core was sieved through 1-mm mesh, and *A. succinea* individuals from each core were counted and killed using carbonated water, and wet weight and length were measured.

Oxygen measurement system

We used a planar optode to simultaneously measure oxygen levels within the burrow and in the sediment of the burrow walls with high spatial and temporal resolution over a period of hours and thus determined how the flux of oxygen into the burrow wall fluctuates over time. Oxygen concentration in a two-dimensional plane was measured using a planar optode system (PreSens GmbH, Regensburg, Germany) that performs ratiometric luminescence imaging of oxygen. The system consisted of thin, fluorescent, oxygen-sensitive foils (SF-RPSu4) and a detector unit (DU01). The foils consist of three layers. (1) An optical isolation layer to prevent color or fluorescent interference from the sample. This layer is 20–50 μm thick,

oxygen-transparent but not reactive, and in direct contact with the sample. (2) An oxygen-sensitive layer with the two fluorescing dyes. This layer is 6–8 μm thick. (3) A support layer that the oxygen-sensitive layer is attached to. This layer is transparent and is attached to the wall of the aquarium. The system is described in Hofmann et al. (2013). The oxygen-sensitive layer is coated with two dyes. One dye emits red light with a wavelength that peaks at 650 nm when excited by violet light (400–420 nm wavelength); the other dye emits green light that peaks at 510 nm when excited by violet light. Oxygen molecules quench the emission of the red-emitting dye but do not interact with the green-emitting dye. Importantly, the sensors consume no oxygen, can be used repeatedly, and offer long-term stability. The response time of the foils is 30 s or less. Because both large changes in burrow oxygen levels and burrow ventilation activities occur over several minutes, this response time should be adequate.

The detector unit provides epi-illumination of the foil with blue led lights, and also detects the emitted light with an enhanced color CMOS chip (a type of RGB chip). Images were digitally recorded through a USB connection on a laptop PC as PNG files. The detector unit's sampling rate and exposure settings were controlled by software provided by the company (VisiSens AnalytiCal 1). The exposure was kept constant throughout all recordings.

We performed a two-point calibration for the sensor foil, at 0 % O_2 saturation and 100 % O_2 saturation. The 0 % calibration measured the red/green ratio in anoxic sediment, and the 100 % saturation calibration measured the red/green ratio in air saturated distilled water mixed with Instant Ocean to a salinity of 35. The average red/green ratio of pixels in a small area in each calibration image was used. The two-point calibration was performed at 6, 24 and 33 °C.

A custom MATLAB program (MathWorks Inc., USA) was used to convert RGB images to oxygen concentration. For each image in the recording, the calibration curve was applied to the ratio of red/green in each pixel of the PNG images to calculate the oxygen saturation. We converted air saturation values to O_2 concentration using the solubility of O_2 in water at salinity 35 at the appropriate temperature.

Experimental setup

Experiments were performed in a narrow glass aquarium (20 × 20 × 5 cm) filled with marine sediment to approximately 5 cm from the top, and topped with aerated seawater (Fig. 1). The O_2-sensitive foils were 4 × 4 cm squares, but for some experiments these were cut into four 2 × 2 cm squares. The foils were affixed to the inside of the glass aquaria with silicon glue approximately 5 cm below the surface of the sediment. Foils could be and were reused

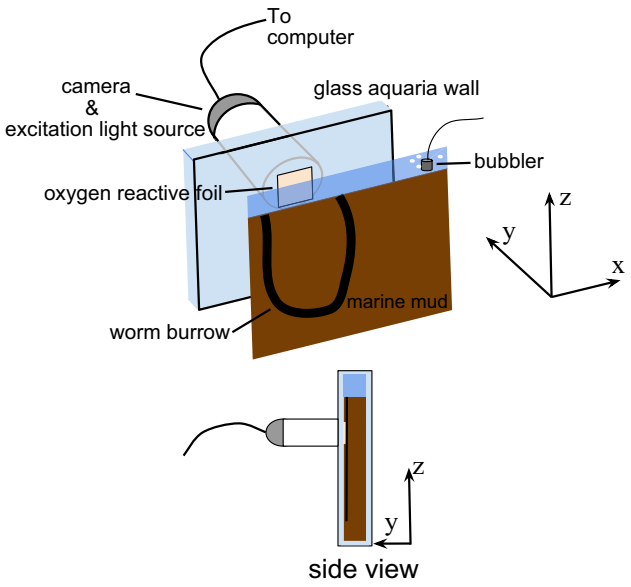

Fig. 1 Experimental setup. Not to scale. An oxygen-sensitive foil was glued to the inside wall of a narrow glass aquaria (20 × 20 × 5 cm) which was filled with muddy marine sediment with overlying, oxygenated seawater. An *Alitta succinea* individual was placed in the aquaria, and built a burrow along the wall behind the foil. The foil was excited with violet light, and the emission from the foil was recorded with the camera

between experiments; however, if they were damaged during the removal of sediment from the aquaria, they were replaced with a new foil. Care was taken during application of the foil to avoid any air bubbles between the foil and the aquarium wall.

A worm was introduced to the aquarium after sediment had been inserted and was allowed to burrow into the sediment near the wall of the aquarium. Likely due to altered mechanical properties at the aquarium wall (Dorgan et al. 2005), worms tended to build burrows up against the aquarium wall. However, when the animal did not construct a burrow behind an oxygen foil new worms were added until one created a burrow behind a foil. Therefore, in some experiments multiple individuals were present in the aquaria prior to recording. This was unlikely to have any effect on recorded oxygen concentrations because oxygen in burrows only diffuses a few millimeters into the sediment. Each recording was made using the same burrow, under the assumption that animals did not switch burrows.

Once an appropriate burrow had been established behind a foil (i.e., the burrow is bisected by the wall of the aquaria) and the worm began ventilation activity, recording was started. Images were taken every 5 or 15 s for 1 to 8 h using the detector unit. Ambient light between the camera and front of the aquarium was blocked using dark piping. The system was also affixed such that the detector unit was at a constant distance from the foil for all experiments. An

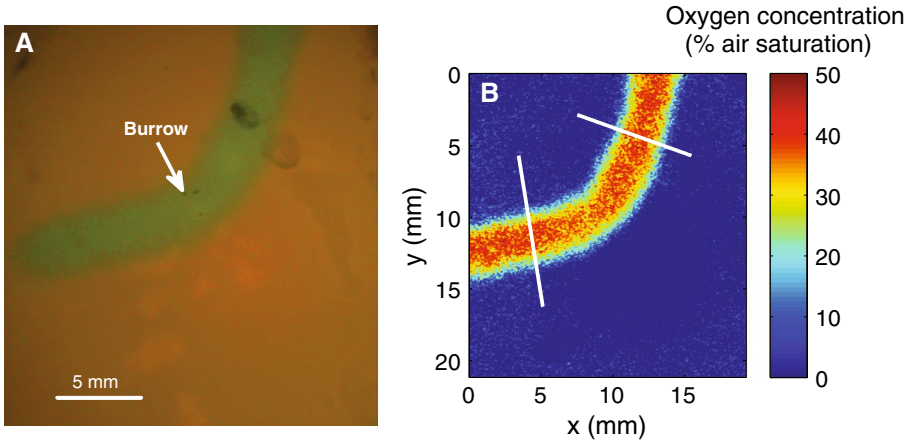

Fig. 2 Example of oxygen data. **a** Image of oxygenated burrow. The burrow is behind an oxygen-sensitive foil that is illuminated with excitation light of a specific wavelength. The burrow is clearly visible in *green* due to a high concentration of dissolved oxygen in the burrow water. The porewater of the surrounding sediment is not green because it is oxygen depleted. The *scale bar* is 5. **b** A calibration curve was applied to every pixel in (**a**). *Warmer colors* indicate higher dissolved oxygen levels. The *white lines* are locations along which oxygen gradients through the burrow and into the burrow wall were calculated

example of an oxygenated burrow recorded by the detector unit is given in Fig. 2a.

Calculation of oxygen flux

Oxygen profiles within the sediment perpendicular to the burrow wall were used to calculate the flux of oxygen from the burrow across the burrow wall, according to Rasmussen and Jørgensen (1992) and Epping and Helder (1997).

The oxygen consumption rate was assumed the same regardless of distance from the burrow wall and that it followed zero-order kinetics (Hall et al. 1989). Sediment porosity was assumed constant with distance from the burrow wall. Results of oxygen gradient measurements in *Hediste diversicolor* burrows by Fenchel (1996) support our assumptions. Additionally, he showed that the burrow walls, lined with a thin layer of mucus, did not impede diffusion of oxygen.

With the above assumptions, and neglecting advective transport, the steady-state concentration of a solute within the sediment is described by the following equation (Epping and Helder 1997):

$$D_s \frac{\partial^2 C(r)}{\partial r^2} - R = 0 \quad (1)$$

where D_s is the porosity corrected diffusivity of oxygen in the sediment; $C(r)$ is the oxygen concentration; r is the radial distance from the burrow wall; and R is the oxygen consumption rate. Although this flux is in the radial dimension, we used a planar coordinate system due to the presence of the planar optode. Therefore,

$$C(r) = \frac{R}{2D_s} r^2 + C_1 r + C_2 \quad (2)$$

where C_1 and C_2 are constants. The oxygen gradient within the sediment was selected perpendicular to the burrow wall from the middle of the burrow to beyond where the oxygen concentration dropped to zero within the sediment (Fig. 2b). Along this line (1 pixel in width), the oxygen concentration was calculated by applying the calibration curve to the red/green ratio at each pixel. The sediment–water interface was determined by locating a distinct change in slope along the oxygen gradient, with a steeper slope within the sediment than in the burrow water (Fenchel 1996). The oxygen concentration profile was determined using a running average of 13 pixels (0.4 mm). To ensure that the middle of the burrow was adjacent to the optode, profiles were only used if a distinct break in the slope of the oxygen concentration at the sediment–water interface within the burrow was observed. In addition, the burrow diameter within optode measurements, with an average of 2.8 ± 0.2 mm, was compared to particle image velocity measurements of excurrent flows obtained at the burrow opening, which had an average burrow openings diameter of 3.2 ± 0.2 mm. This agreement indicated that the optode nearly bisected the burrows for the concentration profiles utilized.

A second-order polynomial was fitted to the smoothed oxygen profile within the sediment:

$$C(r) = ar^2 + br + c \quad (3)$$

where a, b and c are fitting parameters of the parabola. The flux (J) across the burrow wall ($r = 0$) was calculated using Fick's Law (Rutgers van der Loeff et al. 1984):

$$J = -D_s b \quad (4)$$

The diffusion coefficient of oxygen in the sediment was calculated using the relationship presented in Ullman and Aller (1982)

$$D_s = D\varphi^{m-1} \quad (5)$$

where D_s is the diffusivity in sediment, D is the diffusivity of oxygen in water, corrected for temperature and salinity, φ is the porosity and m is an empirically derived constant. We used a value of 3 for m, which Ullman and Aller (1982) determined for sediments with a porosity of 0.7.

Depth of penetration of the oxygen was calculated by locating the vertex of the parabola fitted to the oxygen concentration gradient. The flux was calculated for 9 line transects across the burrow which were parallel and adjacent to each other. Due to the varying lengths of the burrows which formed along the optode, between two and six sets of transects across each burrow were used to calculate the oxygen flux and penetration depth during each time series (Fig. 2b). Transect locations were chosen where a sufficiently clear sediment–water interface at the burrow wall could be found indicating that the optode in this location bisected the burrow. The time series flux data at each location were smoothed using a Savitzky–Golay smoothing function, and the time series oxygen penetration depth was filtered using a Butterworth filter. An example of each data treatment with raw data is provided in Online Resource 1. The dominant frequency of burrow oxygenation and oxygen flux oscillations at each temperature were calculated by a fast Fourier transform (FFT) of the time series. Only recordings lasting 4 or more hours were used.

The limitations of the planar optode system in measuring oxygen concentration gradients around cylindrical objects are discussed in Glud (2008). The presence of the planar optode essentially removes sediment that would otherwise consume oxygen, resulting in a small increase in the measured distance of oxygen penetration and decrease in flux versus what would occur without the presence of the optode (Frederiksen and Glud 2006). In our case, only burrows which were bisected by the optode were used, minimizing this issue, so a correction was not employed (Zhu et al. 2006).

Temperature experiments

Oxygen measurements were taken at 6, 24, and 33 °C, temperatures that are within the seasonal range we observed, with an accuracy of ±1 °C. Animals were first recorded at 24 °C, then at 33 °C and at finally 6 °C. Two individuals were recorded at 24 °C after the 33 °C recording, and the frequency of burrow oxygenation was very similar (within 3.2×10^{-5} Hz) before and after the animal was exposed to heat.

All individuals were held at 24 °C for at least 24 h before recording began. Individuals were not acclimated to the 33 and 6 °C temperatures beyond the time it took for the system to reach the desired temperature (approximately 2 h to reach the cold temperature and 4 h to reach the hot temperature). We did not observe any mortality from either the high- or low-temperature experiments. Note that animals were collected during the summer months, when temperatures ranged between 20 and 34 °C; temperature tended to oscillate around 25 °C on a 12-h cycle. Though we examined the effects of biologically relevant temperatures, acclimatization times to the high and low temperatures were much shorter than would occur in the field.

The 33 °C temperature was achieved using a heat lamp located above and to the side of the aquaria. While a uniform temperature was likely not achieved, we ensured that the temperature of the surface water and the sediment to the depth of the foil was at 33 ± 1 °C. The 6 ± 1 °C temperature was achieved by placing the entire setup in a refrigerator.

Ventilation flow measurements

We measured ventilation flow characteristics using a flow visualization technique, particle image velocimetry (PIV) (Adrian 1991), to measure ventilation flow dynamics. The PIV system (described further in Whitman and Reidenbach 2012) consists of a light sheet that is created by shining a laser (Laserglow Technologies© 300 mW, 532 nm) through a convex lens (Melles Griot© 20° convex lens). The light sheet illuminated neutrally buoyant particles (11-micron silver-coated hollow glass spheres, Potter Industries©) in the water overlying the sediment. The flow field was imaged with a digital camera (Sony High Definition HC7) for 4 h at a frame rate of 30 Hz with a spatial resolution of 620 ± 3 pixels cm^{-1}. We used a hybrid digital PIV technique (Cowen and Monismith 1997) to calculate a vector field of flow velocity in a 512-pixel-high by 256-pixel-wide window directly above a burrow entrance. Cross correlation analysis (Sveen 2004) using MatPIV version 1.6.1 resulted in a velocity field with a resolution of 32 × 32 pixels, or 0.52 × 0.52.

To get the frequency of pumping events over the 4 h of recording, a velocity field was calculated every 5 s a fast Fourier transform (FFT) performed on the average vertical velocity over the burrow. The velocity within the worm burrow was measured as the outflow directly above the burrow entrance. Because laminar flow within a pipe has a parabolic profile across the pipe diameter (Stamhuis and Videler 1998), the flow in the burrow was modeled by fitting a second-order polynomial to the velocity profile across the diameter of the burrow entrance at the sediment–water interface. To calculate the tube flow velocity and volumetric flow rate during

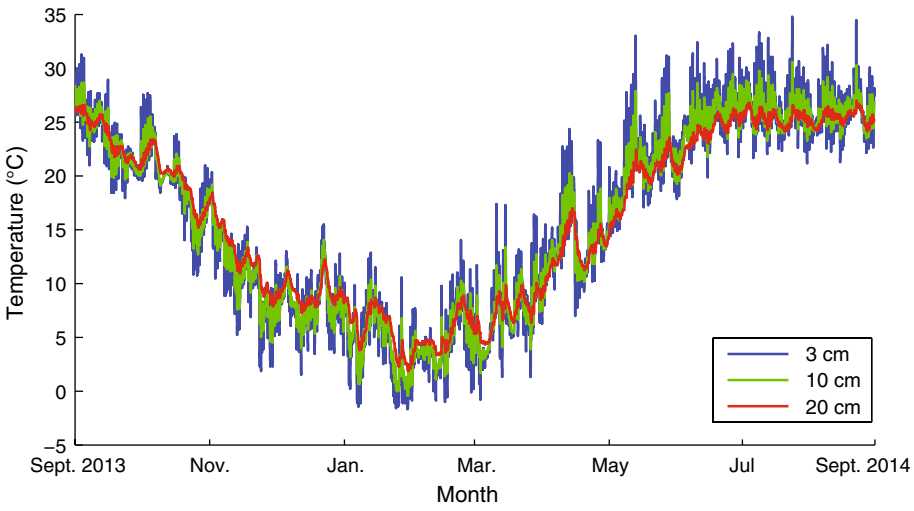

Fig. 3 Year of temperature measurements from three depths in the sediment of an intertidal mudflat. Data are from September 2013 to September 2014. Temperature series shown are from one location. Temperatures were taken at 3, 10 and 20 cm depth in muddy intertidal sediment similar to where *A. succinea* specimens were collected. Temperatures were recorded every 10 min

pumping events, between one and three pumping events were chosen, based upon the orientation of the excurrent flow, and five consecutive instantaneous velocity fields (separated by 1/30th of a second) every 90 s were calculated. The time average of the five consecutive velocity fields was used to calculate the tube flow parameters. The midline velocity is the apex of the parabola, and the mean velocity in the pipe is one half of that. The volumetric flow rate is the mean velocity multiplied by the area of the burrow entrance, and the total volume pumped during a pumping event is the volumetric flow rate integrated over the pumping event duration.

To avoid wall effects on the outflow velocity due to a burrow opening too close to the wall, we glued a false wall of 0.6-cm-thick plexiglass inside the aquarium walls, with the top flush with the sediment surface. This allowed the burrow to be up against the plexiglass false wall, while the burrow opening and excurrent jet were kept away from the glass wall. PIV data could not be collected simultaneously with oxygen data due to interference of the laser used in PIV with the planar optode. Velocity measurements for each individual were recorded at three temperature treatments 9, 24 and 33 °C. The low temperature for this experiment was 2–3 °C higher than that used for the oxygen measurements due to equipment constraints, but this did not appear to affect the behavior response.

Statistics

To analyze the effect of temperature on ventilation parameters and burrow oxygenation, we used a two-way ANOVA testing the effects of individual and temperature. A one-way ANOVA was used to analyze the effect of temperature on the frequency of the oscillation of oxygen flux across the burrow wall. Results are reported as the mean ± 1 standard error, with N as the number of individuals and n as the number of time series analyzed.

Results

Field conditions

While the average temperature was the same at all three sediment depths, shallower depths experienced greater temperature extremes, both high and low. At 3 cm depth, the maximum and minimum recorded temperatures were 33.9 ± 0.9 and −2.1 ± 0.6 °C (number of sites (N) = 3), respectively. The temperatures at 20 cm had very low variance (0.2 ± 0.1 °C) on a 24-h timescale, whereas the temperature at 3 cm depth had higher variance (3.1 ± 0.9 °C) on a 24-h timescale. The variance increased, at all depths, when the timescale over which variance was measured increased (Table 1; Fig. 3).

Alitta succinea abundance

The abundance of *A. succinea* individuals was found to be highly variable in intertidal mudflats. There were between 0 and 6 individuals per 0.05 m^2 sediment sample. One mudflat site had an average of 3.8 ± 1.0 individuals per 0.05 m^2 (76 ± 19 ind. m^{-2}) and the other had an average of 0.4 ± 0.4 individuals per 0.05 m^2 (8 ± 8 ind. m^{-2}). The mean wet weight of *A. succinea* individuals was 0.17 ± 0.02 g (N = 18) and the mean length was 4.9 ± 0.4 cm (N = 16).

Ventilation behavior

At all temperatures, active pumping was intermittent, with the frequency of pumping events increasing tenfold from 9 to 33 °C (Table 2; Fig. 4). The time-averaged volumetric flow rate increased with temperature (two-way ANOVA, $F(2,2) = 13.62$; $P = 0.0003$, $n = 22$, $N = 3$). During active pumping events, the instantaneous maximum volumetric

Table 2 Burrow ventilation flow velocity and volumetric flow rate during active pumping events

	Ventilation periodicity ($\times 10^{-4}$ Hz)	Time-averaged Q ($cm^3\ h^{-1}$)	Instantaneous maximum Q ($cm^3\ s^{-1}$)	Total flow volume during single pumping event (cm^3)	Duration of single pumping event (s)
9 °C ($n = 6$)	1.8 ± 0.1	101 ± 43	0.16 ± 0.07	18.0 ± 11.0	255 ± 90
24 °C ($n = 9$)	15.0 ± 2.2	248 ± 22	0.23 ± 0.04	35.7 ± 16.7	296 ± 19
33 °C ($n = 7$)	18.2 ± 0.7	338 ± 130	0.22 ± 0.06	20.4 ± 4.6	258.9 ± 57.7

$N = 3$ individuals, with n being the number of pumping events analyzed. Q is the volumetric flow rate

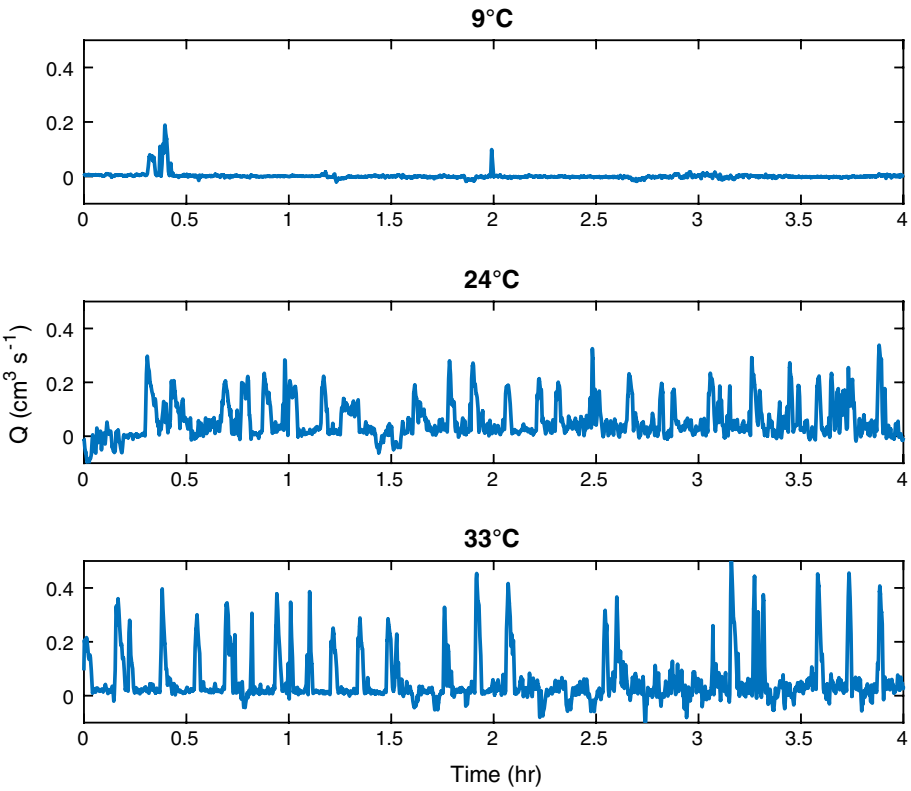

Fig. 4 Volumetric flow rate (Q) over time, at three temperatures. All data are from one individual. The velocity field from which Q was calculated was measured at a frequency of 30 Hz for the entire 4 h, and Q was smoothed using a moving average with a window of 15 s

flow, the volumetric flow rate and the total flow volume, and the duration of pumping events did not exhibit a trend with temperature (Table 2; Fig. 4). The total flow volume ejected from the burrow during a single period of active ventilation was similar at 9 and 33 °C (18.0 ± 11.0 and 20.4 ± 4.6 cm^3), and increased to 35.7 ± 16.7 cm^3 at 24 °C. The average duration of an active ventilation period showed a similar pattern with temperature as the total flow volume, with similar values at 9 and 33 °C and a small increase in duration at 24 °C (Table 2). A representative example of the velocity field over a burrow is given in Fig. 5.

Burrow oxygen dynamics

As a result of burrow ventilation, each burrow was periodically flushed with oxygenated surface water, while the surrounding sediment was oxygen-depleted (Fig. 2). Burrows contained oxygenated water (defined here as greater than 20 % air saturation) for 98 ± 1.3 % of the time at 24 °C and 60 ± 28 and 54 ± 6 % of the time at 6 and 33 °C, respectively. Oxygen levels in the middle of the burrow periodically rose and fell. Burrow oxygenation varied between 80 ± 20 and 150 ± 20 μM (18 ± 3 and 44 ± 5 % air saturation) at 6 °C and 20 ± 3 and 60 ± 2 μM (11 ± 1 to 32 ± 1 % air saturation) at 33 °C. See Online Resource 2 for burrow oxygenation patterns at the three temperature treatments. Oxygen levels in the burrow fluctuate periodically as a result of periodic irrigation, with drops in oxygen concentration occurring approximately every 15 to 30 min at 24 °C, followed by a steep rise when pumping ensued (Fig. 6). Oxygen diffused into the sediment near the burrow wall and was quickly consumed. Oxygen penetration into the burrow wall varied over time (Fig. 7), and these fluctuations were damped with distance from the

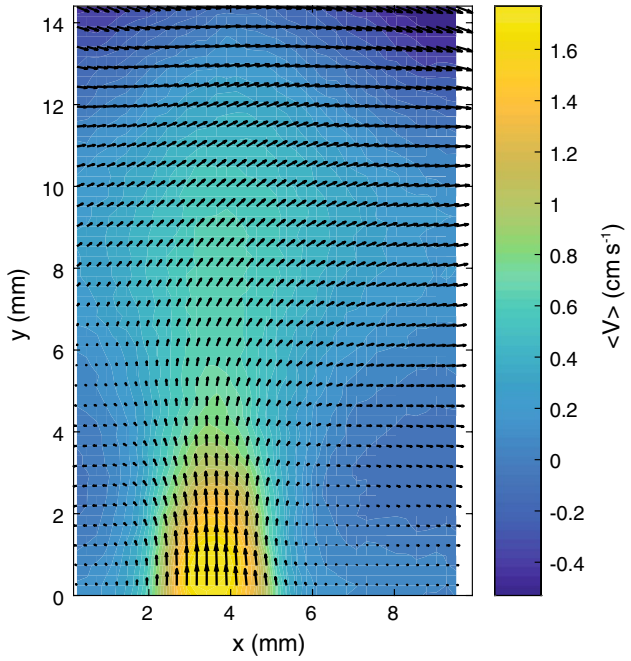

Fig. 5 Time-averaged vertical velocity (<*V*>) during a single ejection event at 24 °C. The length and direction of the *arrows* are relative to the magnitude and direction of the velocity

burrow wall (Fig. 8). The distance that oxygen diffused into the sediment responded to temperature, with a lower temperature resulting in oxygen transport to a greater distance into the sediment (Fig. 9b; Online Resource 3). This effect was significant (two-way ANOVA, $F(2,3) = 31.45$, $P = 0.0097$, $n = 15$) (Table 3).

The flux of oxygen into the sediment across the burrow wall also rose and fell periodically, and tended to follow the pattern of oxygenation (Fig. 6). The periodicity of burrow oxygenation and the flux across the burrow wall varied with temperature. An increase in temperature resulted in an increase in the frequency of burrow oxygenation and flux oscillations (Figs. 8c, d and 9). The effect of temperature on the frequency of burrow oxygenation was significant (two-way ANOVA, $F(2,3) = 37.15$, $P = 0.0026$, $n = 16$). The effect of temperature on the frequency of the flux oscillations was significant (one-way ANOVA, $F(2) = 6.91$, $P = 0.0152$, $n = 12$). However, the average flux across the burrow wall, 1.5 ± 0.3ol m^{-2} d^{-1}, did not respond to temperature (two-way ANOVA, $F(2,3) = 1$, $P = 0.46$, $n = 15$) (Fig. 9a). See Online Resource 3 for more data on oxygen flux periodicity under the three temperature treatments, as well as flux and oxygenation penetration distance data.

Discussion

Burrow oxygenation and oxygen flux

Alitta succinea burrow oxygenation is temporally and spatially heterogeneous due to both ventilation behavior, which

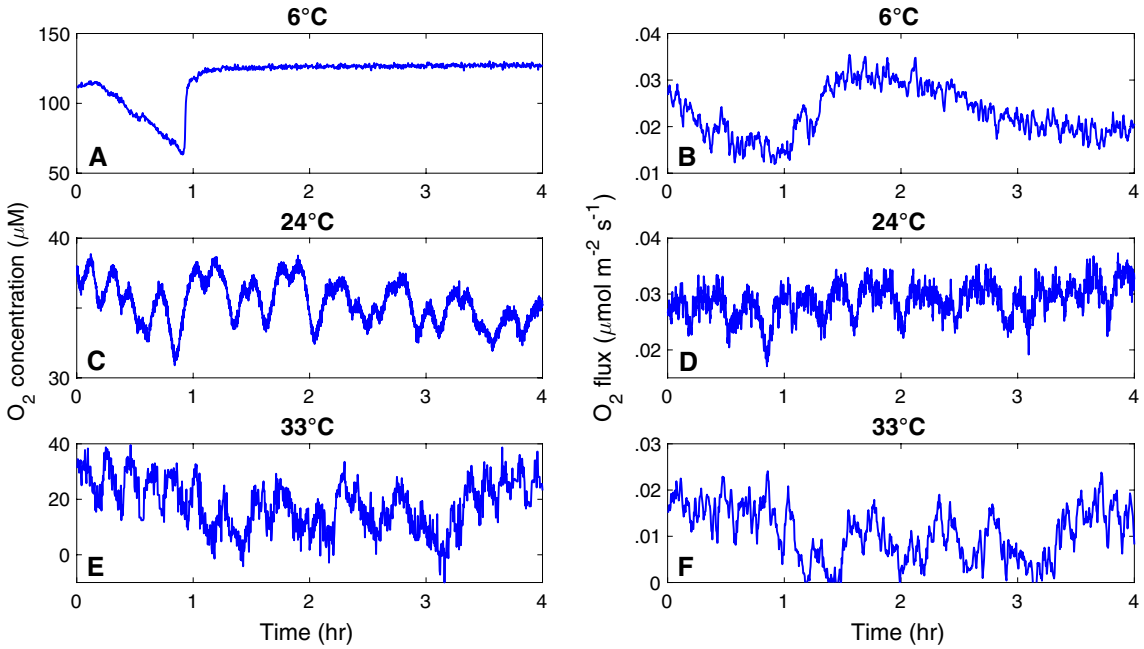

Fig. 6 Oxygen concentration in the middle of a burrow and the corresponding flux across the burrow wall over time, at three temperatures. All data are from one individual. The frequency of oscillations of the flux conforms to the frequency of burrow oxygenation, and the pattern of burrow oxygenation changes with temperature. Please note that the *y*-axes limits are inconsistent between panels, in order to highlight the pattern of the fluctuations

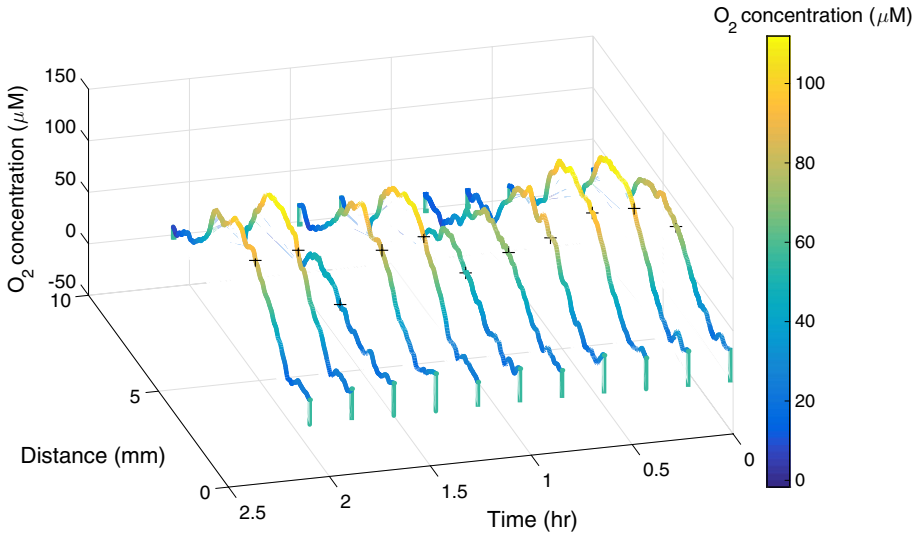

Fig. 7 Changes in oxygen concentration over time along a transect across a burrow and into the sediment. Concentration profiles are an average of 9 pixels (0.28) along the length of the burrow. The profiles were smoothed using a moving average of 13 pixels (0.4 mm). The + *marks* the sediment–water interface at the burrow wall. These measurements were taken at 6 °C

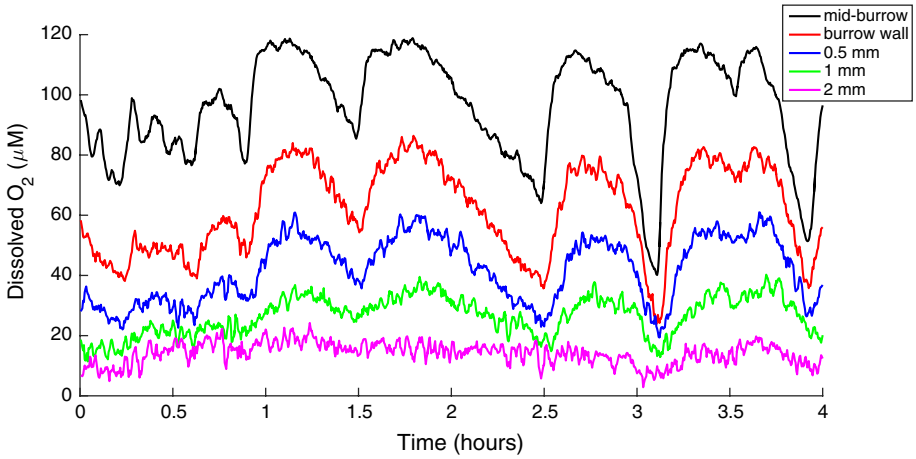

Fig. 8 Oxygen levels within the sediment at different distances from the burrow wall. Data are from a representative sequence. The *black line* shows the oxygen concentration in the burrow water. These measurements were taken at 6 °C

Table 3 Oxygen levels in the sediment adjacent to the burrow walls

Distance from burrow wall (mm)	0	0.5	1	2
Mean oxygen concentration [μM (% air saturation)] ($N = 4$)				
6 °C ($n = 4$)	72 ± 16 (24 ± 5)	59 ± 13 (19 ± 4)	45 ± 11 (15 ± 4)	22 ± 4 (7 ± 1)
24 °C ($n = 6$)	41 ± 5 (19 ± 2)	29 ± 5 (14 ± 2)	20 ± 4 (9 ± 2)	14 ± 4 (6 ± 2)
33 °C ($n = 5$)	13 ± 5 (7 ± 2)	9 ± 4 (5 ± 2)	5 ± 3 (2 ± 2)	2 ± 2 (1 ± 1)

Each sequence is an average of measurements taken from between one and six locations along the burrow. There was at least one sequence at each temperature per individual

Values are mean ± S.E

N the number of individuals, *n* the total number of sequences measurements were taken over

controls the temporal patterns of oxygenation, and fluid dynamics within the burrow: Slower-moving fluid is more depleted of oxygen due to microbial consumption at the burrow wall, as well as diffusion into the sediment. During active pumping, the burrow is flushed with oxygenated water. However, the maximum oxygen concentration in the middle of the burrow averaged 44 ± 5 % air saturation, meaning that oxygen levels in the burrow water are depleted within the burrow. This is similar to levels seen in polychaete and bivalve burrows (Volkenborn et al. 2012a; Fenchel 1996).

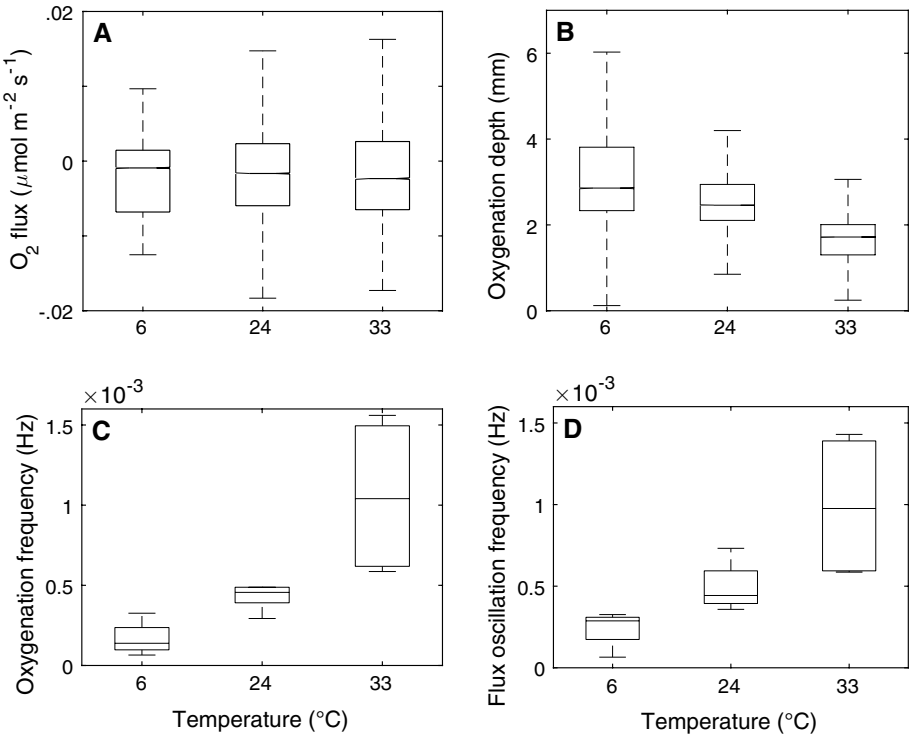

Fig. 9 Box plots summarizing all measurements of the **a** flux, **b** oxygenation distance, **c** oxygenation frequency and **d** oxygen flux oscillation frequency. Flux and oxygenation data were calculated for every frame in every sequence. The total number of hours of oxygen data recorded was 20 h at 6 °C, 24.2 h at 24 °C and 17.8 h at 33 °C. The number of sequences recorded was 4, 6 and 5 for 6, 24 and 33 °C, respectively. $N = 4$ individuals

Our mean oxygen flux value (1.5ol m^{-2} d^{-1}) is comparable to values measured in the burrow of another polychaete, *Hediste diversicolor*. Values ranged from 1.92 ± 0.49 to 3.65 ± 0.80ol m^{-2} d^{-1} depending on the location in the burrow at which the fluxes were measured (Pischedda et al. 2012). In a separate study, oxygen flux across the burrow walls of *H. diversicolor, Nereis virens*, and *Cyclope neritea*, a bivalve, ranged from 5.2 ± 0.8 to 13.3 ± 3.5ol m^{-2} d^{-1}, with similar values in the two polychaete species and higher values in the bivalve burrows (Pischedda et al. 2008). The values for *A. succinea* reported in our study are lower than the values measured for other polychaete species, and may be due in part to shorter pumping durations seen in *A. succinea* (Kristensen 1983), or a result of obstruction of the burrow geometry due to the presence of the optode. Additionally, the maximum fluxes across the burrow wall measured in our study are 2–3 times higher than the average fluxes. This indicates the importance of burrower behavior in controlling the amount of oxygen that is transported into the sediment. The potential flux is higher, but periodic irrigation keeps the oxygen levels in the burrow water and the average flux lower.

The response time of our oxygen-sensitive foils, 30 s or less, possibly convolutes our periodicity measurements. However, a Welch's power spectral density plot (Welch 1967) of the oxygenation data (a measure of the power of the oxygen signal at different frequencies) indicates a noise floor (where noise dominates the signal) at approximately 2 min, meaning that the response time of our foils was at least four times faster than any non-noise fluctuations in oxygen levels. Additionally, the pumping behavior of the worms indicates that changes in ventilation occur on a timescale of minutes, not seconds. For one individual, excurrent velocities were recorded at 30 Hz for a 4-h period across a range of temperatures and smoothed with a moving average window of 15 s (Fig. 4). These measurements indicate the oscillations in pumping occur at or slower than one oscillation every 5 min. This indicates that the response time of the foils gives a sampling frequency of at least two times, but typically greater than the highest frequency non-noise fluctuations we see in the oxygen data.

Sediment oxygen uptake

Burrowing macroinfauna, especially those that build and ventilate burrows, greatly increase the oxygen uptake of sediments due to an increase in diffusive flux across the sediment–water interface and, in more permeable sediment, due to the fact that pumping can induce advective transport into the sediment (Forster et al. 1999; Vopel et al. 2003; Forster and Graf 1995). From our laboratory observations of a 20-cm-deep burrow and assuming a cylindrical U-shaped burrow with a curvature radius of approximately 10 cm, *A. succinea* burrows may typically have a length of up to 50 cm. Given measured diameters of 3 and abundance data we report in the results (up to 120 ind. m^{-2}), this species increases the area of the sediment–water interface by up to 57 %. Given our idealized *A. succinea* burrow, we estimate the average flux into the sediment

per individual burrow to be 7.1 µmol O_2 d^{-1} and an increase in sediment oxygen uptake of 0.8ol O_2 d^{-1} per m^2 of sediment surface due to *A. succinea* ventilation activity. Hume et al. (2011) report a highly variable total oxygen flux into subtidal mudflats ranging from 86.4 to 1010.8ol O_2 m^{-2} d^{-1} in a shallow coastal lagoon near our sediment collection and polychaete sampling sites. Assuming similar oxygen uptake in subtidal and intertidal locations, the ventilation activity of this burrower could account for between 1 and 0.1 % of the total oxygen uptake in these sediments. This is lower than the fauna-mediated oxygen uptake rates reported in other studies; however, this number is highly dependent on burrow size and density of burrows (e.g., *H. diversicolor* burrows contribute between 28 and 92 % of the total oxygen uptake at densities of 450 and 600 ind. m^{-2}, respectively (Wenzhöfer and Glud 2004)). Additionally, these studies include the respiration of the worm itself in oxygen uptake measurements, whereas our study only measured oxygen fluxes into the sediment. Far greater densities of *A. succinea* (1200–1600 ind. m^{-2}) in a coastal lagoon have been reported (Bartoli et al. 2000), where *A. succinea* bioirrigation resulted in sediment oxygen uptake increasing by 31 % at a density of 1660 ind. m^{-2}. At an even higher density (3333 ind. m^{-2}), the presence of *A. succinea* increased sediment oxygen uptake from 12.5 to 52ol m^{-2} d^{-1} (Bosch et al. 2015). Given our oxygen flux results, this density of polychaetes would result, on average, in an additional flux of 23ol O_2 m^{-2} d^{-1} in the sediment.

Burrow ventilation behavior

As found in previous work (Kristensen 1981), *A. succinea* intermittently ventilates its burrow. As we hypothesized, and similarly to what has been observed for burrowing shrimp (Stanzel and Finelli 2004), the frequency of ventilation increased with temperature, likely due to changes in oxygen uptake in the sediment as well as an increase in *A. succinea* metabolism with temperature (Sturdivant et al. 2015). The increase in ventilation velocity and volumetric flow rate with temperature, reported in this study, is also evident for some species of *Thalassinidea* shrimp (Stanzel and Finelli 2004) and several species of nereidid polychaetes (Kristensen 1983). Because these behavior changes occurred after acute exposure, it is difficult to extrapolate these finding to the field. However, our field temperature data show fairly large temperature fluctuations over 12-h timespans (including several instances of an increase of >8 °C), and we observed no behavioral changes over the 4+ h of data collection at the three temperatures.

Temperature effects on oxygen dynamics

Intertidal organisms in Virginia mudflats experience drastic fluctuations in temperature on tidal and seasonal timescales (Fig. 1; Table 1). Temperature has been shown to influence the uptake of oxygen by marine sediments, as well as the depth of oxygenation in sediments, with higher oxygen uptake rates at higher temperatures (Hall et al. 1989) and a shallower layer of oxygenated sediment (Glud et al. 2003). Our laboratory measurements indicate that the frequency of the periodic oscillations in the rate of oxygen flux across the burrow walls increased with temperature. We also found that the average and maximum distance of oxygen penetration from the burrow wall decreased with temperature. This signifies that an increase in temperature results in a smaller volume of sediment that experiences oxic conditions. The temperature dependence of oxygenation depth is likely a result of both oxygen in the sediment being consumed more quickly at a higher temperature (Thamdrup et al. 1998), and lower oxygen values within the burrow at these higher temperatures.

The volumetric consumption of oxygen in the sediment (due to both microbial respiration and redox reactions) can be found using the relationship:

$$R = \frac{J^2}{D_s 2C_0} \tag{6}$$

where C_0 s the concentration of oxygen at the burrow wall ($r = 0$) (Rasmussen and Jorgensen 1992). Volumetric oxygen consumption in our study demonstrated a $Q_{10(6\text{–}33\ ^\circ\text{C})}$ value of 1.9 ± 0.2 ($N = 4$). This is within the range, but at the low end of Q_{10} values (1.5–4.3) previously reported in coastal sediments (Thamdrup et al. 1998 and references therein), which may be due to oxygen availability within the burrow (C_0), being mediated by burrower pumping behavior. Decreased oxygen levels within the burrow, due both to decreased solubility as well as altered pumping behavior and increased burrower metabolism, counteract an increase in microbial metabolism within the sediment. Oxygen solubility [at a salinity of 35, oxygen solubility decreases by 40 % between 6 and 33 °C. (U.S.G.S. 2011)] and the rate of diffusion, consumption of oxygen all change with temperature (Epping and Helder 1997). Thus, the similarity in the magnitude of oxygen fluxes at different temperatures may be because increased oxygen consumption within the sediment at higher temperatures is counteracted by a decrease in oxygen availability within the burrow. This appears to be a result of faster depletion of oxygen within the burrow after the cessation of pumping (Fig. 6). The increase in pumping frequency with temperature may be due to the polychaete attempting to counteract this increased oxygen consumption rate and maintain adequate oxygen levels in the burrow. This may also be compounded by a small decrease in average ventilation duration from the moderate temperature to both the colder and warmer temperatures.

While our results indicate little change in total oxygen flux from worm burrows with temperature, our results suggest a seasonal change in the volume of sediment that experiences oscillating oxygenation conditions due to a burrow. Using the idealized burrow described previously, and the maximum oxygen penetration data we reported, we find that a single burrow would result in a volume of sediment of 26 cm^3 at 33 °C and 90 cm^3 at 6 °C that experiences periodic oxygenation. We would thus expect a maximum of between 3.1×10^{-3} and 11×10^{-3} m^3 of oxygenated sediment due to *A. succinea* burrows per square meter of sediment surface, depending on the temperature.

In conclusion, this study attempts to resolve oxygen dynamics within burrows on small spatial and temporal scales. Periodic burrow ventilation results in similar periodicity in fluxes of oxygen across burrow walls, and the volume of sediment surrounding a burrow that is oxygenated also fluctuates over time. Additionally, the frequency of burrow oxygenation and oxygen flux are temperature dependent, as is the volume of sediment around the burrow that is exposed periodically to oxygen. These results give a detailed understanding of how burrowing organisms mediate the oxygen available to microbes in marine sediment and also show how oxygen availability within sediments surrounding burrows changes with temperature. Here, we show the importance of burrower behavior in linking sediment chemistry with environmental parameters across seasonal timescales.

Acknowledgments The authors wish to thank the staff of the ABCRC, especially D. Boyd and C. Buck, for logistical support. K. Combs and D. Pike assisted with specimen collection. The authors also thank two anonymous reviewers, whose comments substantially improved the manuscript. PreSens Precision Sensing GmbH donated the planar optode system for use in this study. This work was financially supported by the National Science Foundation via a Graduate Research Fellowship to E.A.K.M. and a Grant (NSF-DEB 1237733) to the Virginia Coast Reserve Long Term Ecological Research.

Compliance with ethical standards

Conflict of interest The authors declare they have no conflict of interest.

Human and animals rights All applicable international, national and/or institutional guidelines for the care and use of animals were followed. This article does not contain any studies with human participants performed by any of the authors.

References

Adrian RJ (1991) Particle-imaging techniques for experimental fluid mechanics. Ann Rev Fluid Mech 23:261–304

Aller RC (1994) Bioturbation and remineralization of sedimentary organic matter: effects of redox oscillation. Chem Geol 114:331–345

Aller RC, Aller J (1998) The effect of biogenic irrigation intensity and solute exchange on diagenetic reaction rates in marine sediments. J Mar Res 56:905–936

Bartoli M, Nizzoli D, Welsh DT, Viaroli P (2000) Short-term influence of recolonisation by the polycheate worm *Nereis succinea* on oxygen and nitrogen fluxes and denitrification: a microcosm simulation. Hydrobiologia 431:165–174

Bosch JA, Cornwell JC, Kemp WM (2015) Short-term effects of nereid polychaete size and density on sediment inorganic nitrogen cycling under varying oxygen conditions. Mar Ecol Prog Ser 524:155–169

Boudreau BP, Jørgensen BB (eds) (2001) The benthic boundary layer: transport processes and biogeochemistry. Oxford University Press, New York

Boudreau BP, Marinelli RL (1994) A modelling study of discontinuous biological irrigation. J Mar Res 52(5):947–968

Carlton JT (1979) Introduced invertebrates of San Francisco Bay. In: Conomos TJ (ed) San Francisco Bay: the urbanized estuary. Pacific Division American Association for the Advancement of Science, San Francisco, pp 427–444

Cowen EA, Monismith SG (1997) A hybrid digital particle tracking velocimetry technique. Exp Fluids 22:199–211

D'Andrea AF, DeWitt TH (2009) Geochemical ecosystem engineering by the mud shrimp *Upogebia pugettensis* (Crustacea: Thalassinidae) in Yaquina Bay, Oregon: density-dependent effects on organic matter remineralization and nutrient cycling. Limnol Oceanogr 54(6):1911–1932

Dorgan KM, Jumars PA, Johnson BD, Boudreau BP, Landis E (2005) Burrow extension by crack propagation. Nature 433:475

Dorgan KM, Jumars PA, Johnson BD, Boudreau BP (2006) Macrofaunal burrowing: the medium is the message. Oceanogr Mar Biol 44:85–121

Epping EHG, Helder W (1997) Oxygen budgets calculated from in situ oxygen microprofiles for Northern Adriatic sediments. Cont Shelf Res 17(14):1737–1764

Fenchel T (1996) Worm burrows and oxic microniches in marine sediments. 1. Spatial and temporal scales. Mar Biol 127(2):289–295

Forster S, Graf G (1995) Impact of irrigation on oxygen flux into the sediment: intermittent pumping by *Callianassa subterranea* and "piston-pumping" by *Lanice conchilega*. Mar Biol 123(2):335–346

Forster S, Glud RN, Gundersen JK, Huettel M (1999) In situ study of bromide tracer and oxygen flux in coastal sediments. Estuar Coast Shelf S 49(6):813–827

Frederiksen MS, Glud RN (2006) Oxygen dynamics in the rhizosphere of *Zostera marina*: a two-dimensional planar optode study. Limnol Oceanogr 51:1072–1083

Glud RN (2008) Oxygen dynamics of marine sediments. Mar Biol Res 4:243–289

Glud RN, Gundersen JK, Jørgensen BB, Revsbech NP, Schulz HD (1994) Diffusive and total oxygen uptake of deep-sea sediments in the eastern South Atlantic Ocean: in situ and laboratory measurements. Deep Sea Res Part I 41:1767–1788

Glud RN, Ramsing NB, Gundersen JK, Klimant I (1996) Planar optodes: a new tool for fine scale measurements of two-dimensional O_2 distribution in benthic communities. Mar Ecol Prog Ser 140:217–226

Glud RN, Gundersen JK, Roy H, Jørgensen BB (2003) Seasonal dynamics of benthic O_2 uptake in a semienclosed bay: importance of diffusion and faunal activity. Limnol Oceanogr 48(3):1265–1276

Gundersen JK, Jørgensen BB (1990) Microstructure of diffusive boundary layers and the oxygen uptake of the sea floor. Nature 345:604–607

Hall PO, Anderson LG, van der Loeff MM, Sundby B, Westerlund SF (1989) Oxygen uptake kinetics in the benthic boundary layer. Limnol Oceanogr 34(4):734–746

Henriksen K, Rasmussen MB, Jensen A (1983) Effect of bioturbation on microbial nitrogen transformation in the sediment and fluxes

of ammonium and nitrate to the overlaying water. Ecol Bull 35:193–205
Hofmann J, Meier RJ, Mahnke A, Schatz V, Brackmann F, Trollmann R, Bogdan C, Leibsch G, Wang X, Wolfbeis OS, Jantsch J (2013) Ratiometric luminescence 2D in vivo imaging and monitoring of mouse skin oxygenation. Methods Appl Fluoresc 1:045002
Hume A, Berg P, McGlathery KJ (2011) Dissolved oxygen fluxes and ecosystem metabolism in an eelgrass (*Zostera marina*) meadow measured with the novel eddy correlation technique. Limnol Oceanogr 56:86–96
Janssen F, Huettel M, Witte U (2005) Pore-water advection and solute fluxes in permeable marine sediments (II): benthic respiration at three sandy sites with different permeabilities (German Bight, North Sea). Limnol Oceanogr 50:779–792
Jørgensen BB, Revsbech NP (1985) Diffusive boundary layers and the oxygen uptake of sediments and detritus. Mar Ecol Prog Ser 89:253–267
Karlson K, Hulth S, Ringdahl K, Rosenberg R (2005) Experimental recolonisation of Baltic Sea reduced sediments: survival of benthic macrofauna and effects on nutrient cycling. Mar Ecol Prog Ser 294:35–49
Kristensen E (1981) Direct measurement of ventilation and oxygen uptake in three species of tubicolous polychaetes (*Nereis* spp.). J Comp Physiol 145(1):45–50
Kristensen E (1983) Ventilation and oxygen uptake by three species of *Neries* (Annelida: Polychaeta). II. Effects of temperature and salinity changes. Mar Ecol Prog Ser 12(3):299–306
Kristensen E (1985) Oxygen and inorganic nitrogen exchange in a *Nereis virens* (Polychaeta) bioturbated sediment-water system. J Coast Res 1:109–116
Kristensen E (2000) Organic matter diagenesis at the oxic/anoxic interface in coastal marine sediments, with emphasis on the role of burrowing animals. Hydrobiologia 426(1):1–24
Kristensen E, Kostka JE (2005) Macrofaunal burrows and irrigation in marine sediment: microbiological and biogeochemical interactions. In: Kristensen E, Haese RR, Kostka JE (eds) Interactions between macro- and microorganisms in marine sediments. American Geophysical Union, Washington, D. C., pp 125–158
Kristensen E, Penha-Lopes G, Delefosse M, Valdemarsen T, Quintana CO, Banta GT (2012) What is bioturbation? The need for a precise definition for fauna in aquatic sciences. Mar Ecol Prog Ser 446:285–302
McLoughlin SM (2011) Erosional processes along salt marsh edges on the Eastern Shore of Virginia. Dissertation, University of Virginia, Charlottesville
Meile C, Van Cappellen P (2003) Global estimates of enhanced solute transport in marine sediments. Limnol Oceanogr 48(2):777–786
Papaspyrou S, Gregersen T, Kristensen E, Christensen B, Cox RP (2006) Microbial reaction rates and bacterial communities in sediment surrounding burrows of two nereidid polychaetes (*Nereis diversicolor* and *N. virens*). Mar Biol 148:541–550
Pischedda L, Poggiale JC, Cuny P, Gilbert F (2008) Imaging oxygen distribution in marine sediments: the importance of bioturbation and sediment heterogeneity. Acta Biotheor 56:123–135
Pischedda L, Cuny P, Esteves JL, Poggiale JC, Gilbert F (2012) Spatial oxygen heterogeneity in a *Hediste diversicolor* irrigated burrow. Hydrobiologia 680(1):109–124
Polerecky L, Volkenborn N, Stief P (2006) High temporal resolution oxygen imaging in bioirrigated sediments. Environ Sci Technol 40(18):5763–5769
Rasmussen H, Jørgensen BB (1992) Microelectrode studies of seasonal oxygen uptake in a coastal sediment: role of molecular diffusion. Mar Ecol Prog Ser 81:289–303
Riisgård HU (1989) Properties and energy cost of the muscular piston pump in the suspension feeding polychaete *Chaetopterus variopedatus*. Mar Ecol Prog Ser 56:157–168
Riisgård HU, Larsen PS (2005) Water pumping and analysis of flow in burrowing zoobenthos: an overview. Aquat Ecol 39(2):237–258
Rutgers van der Loeff MM, Anderson LG, Hall POJ, Iverfeldt A, Josefson AB, Sundby B, Westerlund SFG (1984) The asphyxiation technique: an approach to distinguishing between molecular diffusion and biologically mediated transport at the sediment-water interface. Limnol Oceanogr 29(4):675–686
Smee DL, Weissburg MJ (2006) Clamming up: environmental forces diminish the perceptive ability of bivalve prey. Ecology 87(6):1587–1598
Stamhuis EJ, Videler JJ (1998) Burrow ventilation in the tube-dwelling shrimp *Callianassa subterranea* (Decapoda: thalassinidea) II. The flow in the vicinity of the shrimp and the energetic advantages of a laminar non-pulsating ventilation current. J Exp Biol 201(14):2159–2170
Stanzel C, Finelli C (2004) The effects of temperature and salinity on ventilation behavior of two species of ghost shrimp (Thalassinidea) from the northern Gulf of Mexico: a laboratory study. J Exp Mar Biol Ecol 312(1):19–41
Sturdivant SK, Perchik M, Brill RW, Bushnell PG (2015) Metabolic response of the Nereid polychaete, *Alitta succinea*, to hypoxia at two different temperatures. J Exp Mar Biol Ecol 473:161–168
Sveen JK (2004) An introduction to MatPIV v. 1.6. 1. Preprint series. Mechanics and applied mathematics. http://urn.nb.no/URN:NBN:no-23418
Thamdrup B, Hansen JW, Jorgensen BB (1998) Temperature dependence of aerobic respiration in a coastal sediment. Microb Ecol 25:189–200
Ullman WJ, Aller RC (1982) Diffusion coefficients in nearshore marine sediments. Limnol Oceanogr 27:552–556
Volkenborn N, Meile C, Polerecky L, Pilditch CA, Norkko A, Norkko J, Hewitt JE, Thrush SF, Wethey DS, Woodin SA (2012a) Intermittent bioirrigation and oxygen dynamics in permeable sediments: an experimental and modeling study of three tellinid bivalves. J Mar Res 70(6):794–823
Volkenborn N, Polerecky L, Wethey DS, DeWitt TH, Woodin SA (2012b) Hydraulic activities by ghost shrimp *Neotrypaea californiensis* induce oxic-anoxic oscillations in sediments. Mar Ecol Prog Ser 455:141–156
Vopel K, Thistle D, Rosenberg R (2003) Effect of the brittle star *Amphiura filiformis* (Amphiuridae, Echinodermata) on oxygen flux into the sediment. Limnol Oceanogr 48:2034–2045
Welch P (1967) The use of fast Fourier transform for the estimation of power spectra: a method based on time averaging over short, modified periodograms. IEEE Trans Audio Electroacoust 15:70–73
Wells GP, Dales RP (1951) Spontaneous activity patterns in animal behaviour: the irrigation of the burrow in the polychaetes *Chaetopterus variopedatus* Renier and *Nereis diversicolor* OF Müller. J Mar Biol Assoc U K 29(03):661–680
Wenzhöfer F, Glud RN (2004) Small-scale spatial and temporal variability in coastal benthic O_2 dynamics: effects of fauna activity. Limnol Oceanogr 49(5):1471–1481
Whitman ER, Reidenbach MA (2012) Benthic flow environments affect recruitment of *Crassostrea virginica* larvae to an intertidal oyster reef. Mar Ecol Prog Ser 463:177–191
Wilson WH (1990) Competition and predation in marine soft-sediment communities. Annu Rev Ecol Syst 21:221–241
Zhu Q, Aller RC, Fan Y (2006) Two-dimensional pH distributions and dynamics in bioturbated marine sediments. Geochim Cosmochim 70:4933–4949
Ziebis W, Forster S, Huettel M, Jørgensen BB (1996) Complex burrows of the mud shrimp *Callianassa truncata* and their geochemical impact in the sea bed. Nature 382:619–622